Osteoblast-specific expression of Fra-2/AP-1 controls adiponectin and osteocalcin expression and affects metabolism

Aline Bozec[1,2], Latifa Bakiri[1], Maria Jimenez[1], Evan D. Rosen[3], Philip Catalá-Lehnen[4], Thorsten Schinke[4], Georg Schett[2], Michael Amling[4] and Erwin F. Wagner[1,*]

[1]Genes, Development and Disease Group, F-BBVA-CNIO Cancer Cell Biology Program, Spanish National Cancer Research Centre (CNIO), 28029 Madrid, Spain
[2]Department of Medicine 3, Rheumatology and Immunology, University of Erlangen-Nuremberg, Nikolaus-Fiebiger-Zentrum Glueckstrasse 6, 91054 Erlangen, Germany
[3]Division of Endocrinology, Beth Israel Deaconess Medical Center, Boston, MA 02215, USA
[4]Department of Osteology and Biomechanics, University Medical Center, Hamburg-Eppendorf, Martinistrasse 52, 20246 Hamburg, Germany
*Author for correspondence (ewagner@cnio.es)

Accepted 5 August 2013
Journal of Cell Science 126, 5432–5440

doi: 10.1242/jcs.134510

Summary

Recent studies have established that the skeleton functions as an endocrine organ affecting metabolism through the osteoblast-derived hormone osteocalcin (Ocn). However, it is not fully understood how many transcription factors expressed in osteoblasts regulate the endocrine function. Here, we show that mice with osteoblast-specific deletion of Fra-2 (*Fosl2*) have low bone mass but increased body weight. In contrast, transgenic expression of Fra-2 in osteoblasts leads to increased bone mass and decreased body weight accompanied by reduced serum glucose and insulin levels, improved glucose tolerance and insulin sensitivity. In addition, mice lacking Fra-2 have reduced levels of circulating Ocn, but high adiponectin (Adipoq), whereas Fra-2 transgenic mice exhibit high Ocn and low Adipoq levels. Moreover, we found that Adipoq was expressed in osteoblasts and that this expression was transcriptionally repressed by Fra-2. These results demonstrate that Fra-2 expression in osteoblasts represents a novel paradigm for a transcription factor controlling the endocrine function of the skeleton.

Key words: Fra-2, *Fosl2*, Activator protein 1, AP-1, Adiponectin, Metabolism, Osteoblasts, Osteocalcin

Introduction

Bone-forming osteoblasts and mesenchyme-derived adipocytes share common progenitor cells. Adipokines, such as leptin, resistin and adiponectin (Adipoq) are primarily produced by adipocytes and are important regulators of metabolism (Kawai et al., 2009; Shetty et al., 2009). Bone has recently emerged as an endocrine organ regulating glucose metabolism through osteoblast-specific secretion of osteocalcin (Ocn) (Karsenty and Ferron, 2012). Osteoblast-specific expression of the transcription factors FoxO1 and ATF4 regulate glucose and insulin metabolism, energy expenditure and fertility through transcriptional regulation of Esp (osteotesticular protein tyrosine phosphatase) (Rached et al., 2010; Yang and Karsenty, 2004; Yang et al., 2004; Yoshizawa et al., 2009), thus decreasing Ocn decarboxylation (Ferron et al., 2008; Ferron et al., 2010; Oury et al., 2011; Yoshizawa et al., 2009). ATF4 is a member of the activator protein (AP)-1 transcription factor consisting of a variety of dimers composed of members of the Fos, Jun and ATF proteins. In mice loss- and gain-of-function mutations of Fos and ATF members, and to a lesser extent of Jun members, demonstrate that these factors are important for osteoblast differentiation and function (Wagner and Eferl, 2005). Whereas Fra-1 (Fos-related antigen 1, *Fosl1*) and ΔFosB (the short isoform of FosB) promote osteoblast differentiation and activity (Eferl et al., 2004; Kveiborg et al., 2002; Lefterova and Lazar, 2009; Zhao et al., 2008), Fra-2 (Fos-related antigen 2, *Fosl2*) is important in normal physiology and disease, such as in pulmonary fibrosis (Eferl et al., 2008). Fra-2 also regulates chondrocyte differentiation (Karreth et al., 2004) and bone remodeling by controlling osteoclast size and activity (Bozec et al., 2008). Furthermore, Fra-2 controls bone formation by transcriptional regulation of the collagen isoform *Col1a2* and Ocn expression in mouse and human osteoblasts (Bozec et al., 2010). However, the effects of Fra-2 expression beyond bone, for example, on metabolism, have not yet been described.

Here, we show that osteoblast-specific Fra-2 expression regulates Adipoq and Ocn levels, thereby affecting systemic glucose and insulin metabolism. Importantly, Fra-2 expression in osteoblasts represses Adipoq at the transcriptional level. These data provide a new link between the endocrine function of the skeleton and systemic metabolism regulated by AP-1.

Results

Osteoblast-specific Fra-2 expression affects bone formation and Ocn secretion

We generated osteoblast-specific Fra-2 mutant mice to investigate the role of Fra-2 in osteoblasts on bone homeostasis and metabolism. Mice with the *Osx-tTA-Cre* allele were crossed to mice carrying two different Fra-2 alleles to either delete Fra-2

(*Fosl2*$^{\Delta ob}$) or express Fra-2 (*Fosl2*$^{ob\text{-}tet}$) in osteoblasts (Rodda and McMahon, 2006). Both mutant mice were maintained without doxycycline to allow Fra-2 deletion or transgene expression during development. Bones of *Fosl2*$^{\Delta ob}$ mutants expressed lower levels of Fra-2 mRNA and protein, whereas *Fosl2*$^{ob\text{-}tet}$ mice expressed higher levels of Fra-2 (supplementary material Fig. S1a–f). No change in Fra-2 mRNA or protein expression was detected in other organs, such as pancreas, muscle, liver or inguinal fat pad in either *Fosl2*$^{\Delta ob}$ or *Fosl2*$^{ob\text{-}tet}$ mice (supplementary material Fig. S1a–f). Furthermore, immunohistochemical stainings of Fra-2 in long bones showed increased Fra-2 expression in osteoblasts and chondrocytes in *Fosl2*$^{ob\text{-}tet}$ mice, whereas in *Fosl2*$^{\Delta ob}$ mice, Fra-2 staining was hardly detectable (supplementary material Fig. S1c,d). This indicates that Fra-2 expression or deletion is restricted to mesenchymal cells of the bone compartment.

Histomorphometric analyses of bones from two-month-old *Fosl2*$^{\Delta ob}$ mice revealed a decrease in bone volume, trabecular thickness and number, whereas an increase in these parameters was observed in *Fosl2*$^{ob\text{-}tet}$ mice (Fig. 1A,B). *Fosl2*$^{\Delta ob}$ mice displayed a decrease in osteoblast surface, whereas osteoclast surface was increased, suggesting disturbed bone homeostasis (Fig. 1A). In contrast, *Fosl2*$^{ob\text{-}tet}$ mice displayed increased osteoblast surface and decreased osteoclast surface (Fig. 1B). Adipocyte number and size were similar in control and *Fosl2*$^{\Delta ob}$ or *Fosl2*$^{ob\text{-}tet}$ tibia (supplementary material Fig. S2a,b). Bone formation assessed by calcein labeling was decreased in *Fosl2*$^{\Delta ob}$ mice and increased in *Fosl2*$^{ob\text{-}tet}$ animals, whereas, no statistical difference in resorption defined by serum CTX could be detected in the two mutant strains (Fig. 1A,B). Furthermore, expression of type 1 collagens and Ocn were decreased in *Fosl2*$^{\Delta ob}$ long bones and increased in *Fosl2*$^{ob\text{-}tet}$ long bones (Fig. 1C,D). Circulating levels of Ocn were decreased in *Fosl2*$^{\Delta ob}$ mice and increased in *Fosl2*$^{ob\text{-}tet}$ mice (Fig. 1E). These data indicate that changes in the bone-forming activity of osteoblasts are responsible for the low and high bone mass phenotype observed in Fra-2 mutant mice. *In vitro* differentiation experiments were next performed to analyze whether the bone phenotype was cell autonomous. Osteoclast differentiation and osteoclast marker expression, such as Acp5 (also known as TRAP) and cathepsin K, were not altered (supplementary material Fig. S3a–c). *Fosl2*$^{\Delta ob}$ primary osteoblasts produced fewer mineralized nodules, when cultured in osteogenic conditions, whereas increased nodule formation was observed in *Fosl2*$^{ob\text{-}tet}$ cultures (supplementary material Fig. S4a,c). In addition, collagen content, and *Col1a1*, *Col1a2* and *Ocn* mRNA levels were decreased in *Fosl2*$^{\Delta ob}$ cultures and increased in *Fosl2*$^{ob\text{-}tet}$ cultures (supplementary material Fig. S4a–d). To determine whether adipocytes, which share common precursors with osteoblasts were altered, mesenchymal progenitors isolated from *Fosl2*$^{ob\text{-}tet}$ and *Fosl2*$^{\Delta ob}$ calvariae

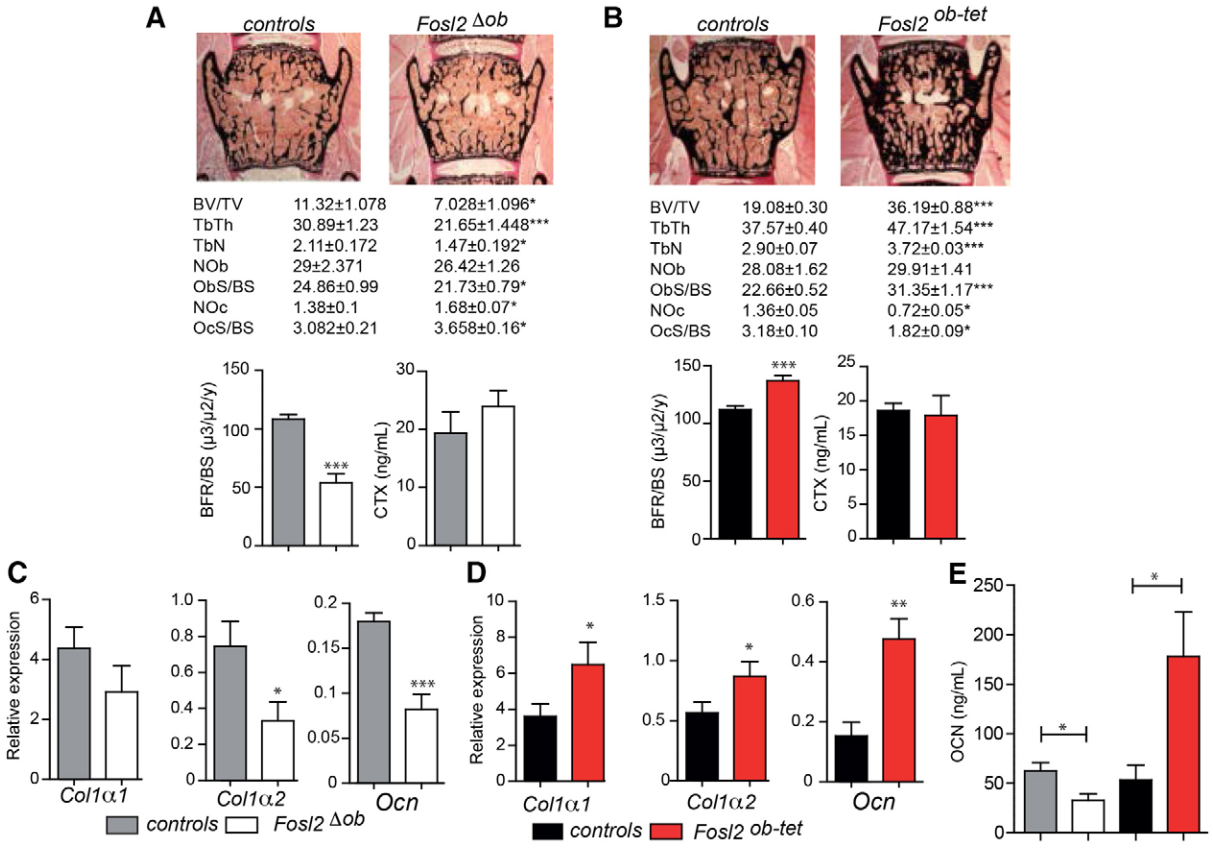

Fig. 1. Bone phenotypes in osteoblast-specific Fra-2 mutant mice. (A,B) Von Kossa staining of spines, and quantification of bone volume (BV/TV), trabecular bone surface (TbTh), trabecular number (TbN), osteoblast number (NOb), osteoblast surface per bone surface (ObS/BS), osteoclast number (NOc), osteoclast surface per bone surface (OcS/BS), bone formation rate per bone surface (BFR/BS) and CTX levels in *Fosl2*$^{\Delta ob}$ (A) and *Fosl2*$^{ob\text{-}tet}$ (B) mice at 2 months of age (n=8). (C,D) qPCR analyses of *Col1a1*, *Col1a2* and *Ocn* in *Fosl2*$^{\Delta ob}$ (C) and *Fosl2*$^{ob\text{-}tet}$ (D) long bones at 3 months of age (n=6). (E) Total Ocn levels in sera from controls and *Fosl2*$^{\Delta ob}$ or *Fosl2*$^{ob\text{-}tet}$ mice at 3 months of age; error bars represent s.d. (n=6). *P<0.05, **P<0.01, ***P<0.001.

were differentiated into adipocytes. Oil Red O staining and expression analyses of peroxisome proliferator-activated receptor γ (PPARγ) and CCAAT/enhancer-binding protein α (CEBPα), early adipocyte markers, revealed a comparable adipogenic potential of *Fosl2*$^{\Delta ob}$ and *Fosl2*$^{ob\text{-}tet}$ cells when compared to control cells, whereas these markers were hardly detectable in osteoblast cultures (supplementary material Fig. S5a–c). These data demonstrate that genetic manipulation of Fra-2 in osteoblasts specifically affects the bone-forming activity of the osteoblast lineage.

Fra-2 expression in osteoblasts controls Adipoq production

Fra-2 was recently shown to control leptin expression in adipocytes (Wrann et al., 2012). We therefore measured the levels of serum adipokines and Ocn isoforms in Fra-2 mutant mice. No changes were observed for leptin and resistin (supplementary material Fig. S6a,b), whereas using the hydroxyapatite (HA) assay followed by enzyme-linked immunosorbent assay (ELISA), total, carboxylated and undercarboxylated Ocn levels were decreased in *Fosl2*$^{\Delta ob}$ sera and increased in *Fosl2*$^{ob\text{-}tet}$ sera (supplementary material Fig. S6c,d). Interestingly, total Adipoq levels were significantly increased in *Fosl2*$^{\Delta ob}$ sera and decreased in *Fosl2*$^{ob\text{-}tet}$ sera (Fig. 2A,B). Moreover, the high molecular weight (HMW) Adipoq, which is the active form (Tilg and Moschen, 2006) as well as the low (LMW) and middle molecular weight (MMW) forms of Adipoq with less defined functions (Takeda et al., 2002) were similarly altered (Fig. 2A,B). Surprisingly, Adipoq

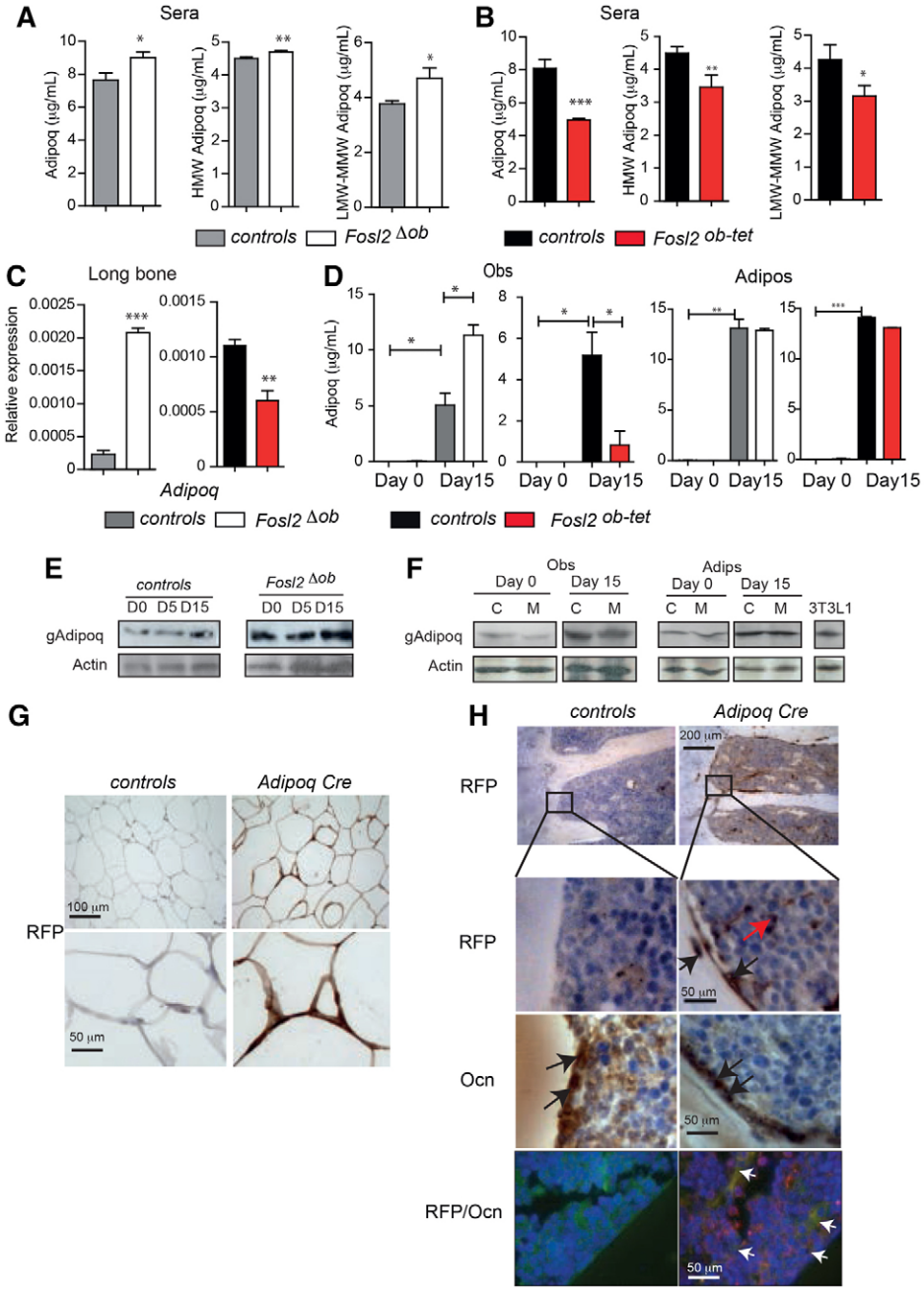

Fig. 2. Adiponectin expression in osteoblasts is altered in Fra-2 mutant mice. (A,B) Total Adipoq, high molecular weight (HMW) Adipoq and low and middle molecular weight (LMW-MMW) Adipoq levels in sera from *Fosl2*$^{\Delta ob}$ (A) and *Fosl2*$^{ob\text{-}tet}$ (B) mice at 3 months of age; error bars represent s.d. (n=6 or 7). (C) qPCR analyses of *Adipoq* in bone from *Fosl2*$^{\Delta ob}$ or *Fosl2*$^{ob\text{-}tet}$ mice (n=6). (D) Adipoq levels in supernatants from controls and *Fosl2*$^{\Delta ob}$ or *Fosl2*$^{ob\text{-}tet}$ osteoblasts (Obs) or adipocytes (Adipos) following differentiation at day 0 and 15 after addition of β-glycerophosphate and ascorbic acid or insulin; error bars represent s.d. (n=6). (E) Western blot analyses of globular Adipoq (gAdipoq) in controls and *Fosl2*$^{\Delta ob}$ osteoblasts at day 0, days 5 and 15 of in vitro differentiation. (F) Western blot analyses of globular Adipoq (gAdipoq) in controls and *Fosl2*$^{ob\text{-}tet}$ osteoblasts or adipocytes at day 0 and day 15 of *in vitro* differentiation, with 3T3L1 cells as positive controls. (G) Immunohistochemical analyses of RFP in controls and *Adipoq Cre* fat pad. (H) Immunohistochemical analyses of RFP and Ocn staining in controls and *Adipoq Cre* long bones. Black arrows indicate osteoblasts; red arrows indicate adipocytes. The lower panels show co-immunofluorescence with Texas Red for RFP, FITC for Ocn and DAPI staining for nucleus in controls and *Adipoq Cre* long bones; co-expression of RFP and Ocn appears yellow and is indicated by white arrows. *P<0.05, **P<0.01, ***P<0.001.

expression was unchanged in its main production site, the adipose tissue of *Fosl2*$^{ob\text{-}tet}$ or *Fosl2*$^{\Delta ob}$ mice (supplementary material Fig. S6e). Interestingly, we found that *Adipoq* mRNA levels were increased in long bones of *Fosl2*$^{\Delta ob}$ and decreased in *Fosl2*$^{ob\text{-}tet}$ mice, suggesting that Adipoq can be produced in bone cells (Fig. 2C). To determine which cells can express Adipoq in long bones, Adipoq production and expression were measured in *Fosl2*$^{ob\text{-}tet}$ and *Fosl2*$^{\Delta ob}$ primary cells cultured in osteogenic or adipogenic conditions. Despite a lower level of Adipoq mRNA and protein in osteoblast cultures compared to adipocyte cultures, Adipoq production and expression by mineralized osteoblasts was increased in the absence of Fra-2 and decreased in Fra-2 overexpressing cells, whereas no difference was observed in cells cultured in adipogenic conditions (Fig. 2D; supplementary material Fig. S6f,g). These findings were confirmed by western blot analyses (Fig. 2E,F).

Moreover, sections from transgenic reporter mice (Adipoq-cre; ROSA26-lox-stop-lox-RFP) were stained for red fluorescent protein (RFP) and Ocn (Eguchi et al., 2011). Positive staining for RFP was observed in Adipoq-cre reporter fat cells (Fig. 2G). Interestingly, osteoblasts, osteocytes and adipocytes were positively stained in Adipoq-cre reporter long bone sections (Fig. 2H). Importantly, the RFP staining was localized to areas positive for Ocn staining on subsequent sections (Fig. 2H). Moreover, co-immunofluorescence analyses showed co-expression of RFP and Ocn in long bones (Fig. 2H). These results indicate that bone is a potential source of Adipoq and that Adipoq expression and secretion by osteoblasts is Fra-2 dependent.

Fra-2 transcriptionally represses *Adipoq*

To determine whether Fra-2 controls *Adipoq* transcription in osteoblasts, a 5 kb *Adipoq* promoter fragment, which includes a putative non-consensus binding region for Fra-2 at position −3.8 kb, was analyzed. Using chromatin immunoprecipitation (ChIP), with anti-Fra-2 antibodies on *Fosl2* control and knockout primary osteoblasts, Fra-2 binding at this site was observed (Fig. 3A). To further characterize the specificity and potential dimerizing partners of Fra-2 on the *Adipoq* promoter, ChIP was

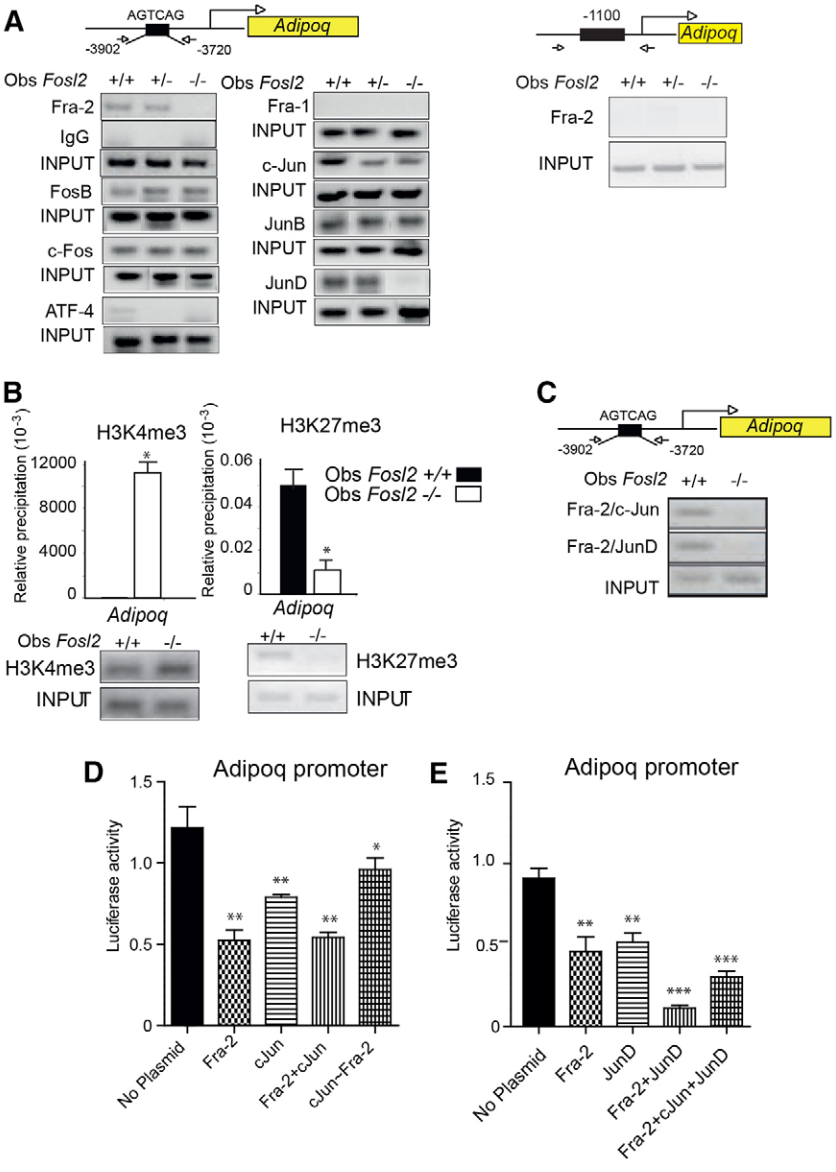

Fig. 3. Fra-2 transcriptionally represses adiponectin in osteoblasts. (A) ChIP of AP-1 proteins at the *Adipoq* promoter; arrows indicate primers used for amplifying fragments at the AGTCAG site. Chromatin of the indicated genotypes was immunoprecipitated with antibodies against IgG, Fra-2, FosB, c-Fos, ATF4, Fra-1, c-Jun, JunB and JunD and end-point qPCR fragments are shown (left panel). Chromatin of the indicated genotypes was immunoprecipitated with Fra-2 for the localization −1100 of Adipoq promoter (right panel). (B) H3K4me3 and H3K27me3 ChIP on Adipoq promoter; chromatin from osteoblasts of the indicated genotypes was immunoprecipitated with H3K4me3 and H3K27me3-specific antibodies, end-point qPCR fragments are shown (n=3). (C) ChIP-on-ChIP of AP-1 proteins at the *Adipoq* promoter. Chromatin of the indicated genotypes was immunoprecipitated with Fra-2 and then antibodies against c-Jun or JunD, and end-point qPCR-fragments are shown (n=2). (D) Luciferase assay on fragments containing the AGTCAG site from the promoter. Luciferase assays were performed with plasmids expressing Fra-2, c-Jun, Fra-2 plus c-Jun or the dimer c-Jun–Fra-2; error bars represent s.d. (n=3). (E) Luciferase assay on fragments containing the AGTCAG site from the Adipoq promoter. Luciferase assays on Adipoq promoter were performed with plasmids expressing Fra-2, JunD, Fra-2 plus JunD, or Fra-2 plus c-Jun plus JunD; error bars represent s.d. (n=3). *P<0.05, **P<0.01, ***P<0.001.

performed for IgG and other AP-1 transcription factors. *Fosl2*-knockout osteoblasts were used as a control for Fra-2 antibody specificity and to identify the dimerization partner of Fra-2. No binding of IgG, ATF-4 and Fra-1 to the *Adipoq* promoter could be detected and Fra-2 did not bind a region around −1100 (Fig. 3A). However, FosB, c-Fos and JunB could bind the *Adipoq* promoter in the presence or absence of Fra-2 (Fig. 3A). JunD and c-Jun clearly bound the *Adipoq* promoter in wild-type cells, whereas decreased binding of c-Jun and no binding of JunD was detected in the absence of Fra-2, suggesting that in osteoblasts c-Jun and JunD probably bind to this fragment as a heterodimer with Fra-2 (Fig. 3A). Additional ChIP assays were performed with antibodies directed against methylated histone H3 to analyze chromatin modifications on the *Adipoq* promoter (Fig. 3B). ChIP and quantitative PCR (qPCR) analyses of the *Adipoq* promoter revealed high levels of active (H3K4me3) and decreased repressive (H3K27me3) methylation marks in Fra-2-deficient cells. This indicates that the *Adipoq* promoter was more active in the absence of Fra-2 (Fig. 3B). ChIP on ChIP Fra-2 and c-Jun, and Fra-2 and JunD confirmed that c-Jun and JunD might be the dimerizing partner of Fra-2 on the *Adipoq* promoter because in the absence of Fra-2, neither c-Jun nor JunD antibodies were able to pull down the *Adipoq* promoter chromatin fragment (Fig. 3C). In addition, *Adipoq* promoter activity assessed by luciferase assay was decreased by the addition of Fra-2, c-Jun, JunD or a combination of these three AP-1 members, confirming that these factors are repressing *Adipoq* expression (Fig. 3D,E). These data demonstrate that Fra-2 can repress *Adipoq* transcription in osteoblasts.

Altered body mass and glucose metabolism in osteoblast-specific Fra-2 mutant mice

Because Ocn and Adipoq are important regulators of metabolism, we next analyzed the metabolic parameters of osteoblast-specific Fra-2 mutant mice. Six-week-old mice were placed on a normal diet (ND) or on a high fat diet (HFD) for six weeks. $Fosl2^{\Delta ob}$ mice were heavier under both ND and HFD conditions with an increased gonadal fat pad weight (Fig. 4A), whereas $Fosl2^{ob\text{-}tet}$ mice were leaner with decreased weight and decreased fat pad weight under both conditions (Fig. 4B). Insulin and glucose levels were next analyzed. Although mild difference in glucose and insulin levels could be detected in $Fosl2^{\Delta ob}$ mice (Fig. 4C,D), $Fosl2^{ob\text{-}tet}$ mice had lower serum glucose levels and lower circulating insulin compared to controls under all tested conditions (Fig. 4E,F). In addition, glucose-stimulated insulin secretion tests (GSIS) indicated that the relative insulin response to glucose stimulation was higher in $Fosl2^{ob\text{-}tet}$ mice (supplementary material Fig. S7a). Insulin content was next measured in $Fosl2^{ob\text{-}tet}$ bones and pancreata. Bone insulin content was not altered, whereas insulin content was decreased in $Fosl2^{ob\text{-}tet}$ pancreata, suggesting a defect in insulin synthesis (supplementary material Fig. S7b). To further analyze glucose and insulin metabolism, glucose (GTT) and insulin (ITT) tolerance tests were employed. A decrease in glucose tolerance and insulin sensitivity was observed in $Fosl2^{\Delta ob}$ mice compared to littermate controls in ND and HFD conditions (Fig. 4G; supplementary material Fig. S7c). In contrast, $Fosl2^{ob\text{-}tet}$ mice showed a remarkable increase in glucose tolerance and insulin sensitivity in both conditions (Fig. 4H; supplementary material Fig. S7d). Moreover, an insulin-induced increase of phosphorylated AKT (pAKT) was attenuated in $Fosl2^{\Delta ob}$, but increased in $Fosl2^{ob\text{-}tet}$ fat, liver and muscle (supplementary material Fig. S7e–g). These data demonstrate that Fra-2 expression in osteoblasts altered insulin and glucose responses, probably through affecting Ocn and Adipoq levels.

Finally, intravenous injections of adenoviruses expressing Adipoq (Ad-Adipoq) partially rescued the metabolic phenotype in $Fosl2^{ob\text{-}tet}$ mice. The levels of circulating Adipoq were increased and similar in $Fosl2^{ob\text{-}tet}$ and littermate control mice under a ND, when compared to PBS- or Ad-Empty-injected mice (supplementary material Fig. S8a). In addition, the levels of Ocn remained higher in $Fosl2^{ob\text{-}tet}$ mice under all conditions (supplementary material Fig. S8b). This suggests that Ad-Adipoq injection can only modify the Adipoq levels within the physiological range without affecting Ocn secretion, allowing us to discriminate between the role of Adipoq and Ocn in our model. The weight of $Fosl2^{ob\text{-}tet}$ mice after Ad-Adipoq injection remained lower than the weight of control mice, although the decrease did not reach statistical significance under a HFD (supplementary material Fig. S8c). Fat pad weight in ND was similar to controls after Ad-Adipoq injection (supplementary material Fig. S8d), whereas a lower fat pad weight was still observed under a HFD (supplementary material Fig. S8d). This suggests that Ocn is probably responsible for the remaining body and fat pad weight alterations observed in $Fosl2^{ob\text{-}tet}$ mice. Importantly, glucose and insulin levels were comparable between mutant and control mice after Ad-Adipoq treatment in ND (supplementary material Fig. S8e,f). Under HFD, the levels of insulin remained lower in $Fosl2^{ob\text{-}tet}$ mice, whereas glucose levels were restored (supplementary material Fig. S8d,e,f). GTT and ITT assays revealed a complete rescue of glucose and insulin handling in Ad-Adipoq-injected mice under ND (supplementary material Fig. S8g,h). In HFD after Ad-Adipoq injection, despite a slight increased insulin sensitivity persisting in $Fosl2^{ob\text{-}tet}$ mice, Ad-Adipoq-injected mice had a similar response to glucose (data not shown). These data support our notion that osteoblast-specific Fra-2 expression can regulate glucose metabolism and that Adipoq produced by osteoblasts contributes to the defects in glucose and insulin handling.

Discussion

In this report, we have shown a new endocrine role for osteoblast-specific Fra-2 expression, which regulates the transcription of *Adipoq* and *Ocn* leading to altered bone physiology and metabolic responses (Fig. 4I). Ocn (Bozec et al., 2010) and *Adipoq* were found to be transcriptionally regulated by Fra-2. The expression of Fra-2 in osteoblasts induced a leaner phenotype, lower glucose and insulin levels, an improved glucose response and insulin sensitivity in $Fosl2^{ob\text{-}tet}$ mice.

Fos proteins have multiple functions in normal bone physiology, regulating bone mass through cell autonomous control of osteoblast differentiation (Bozec et al., 2010; Eferl et al., 2004; Grigoriadis et al., 1993). Distinct target genes are regulated by the Fos-related proteins Fra-1 and Fra-2, which control osteoblast differentiation and activity, rather than osteoblast numbers (Bozec et al., 2010; Eferl et al., 2004). Fra-2 transcriptionally regulates leptin, which can control energy homeostasis in mesenchymal cells (Wrann et al., 2012). Surprisingly, leptin was not affected in Fra-2 mutant mice, whereas the levels of the adipokine Adipoq were found to be altered in Fra-2 mutant sera. Adipoq is known to enhance the action of insulin by several mechanisms, including suppression of

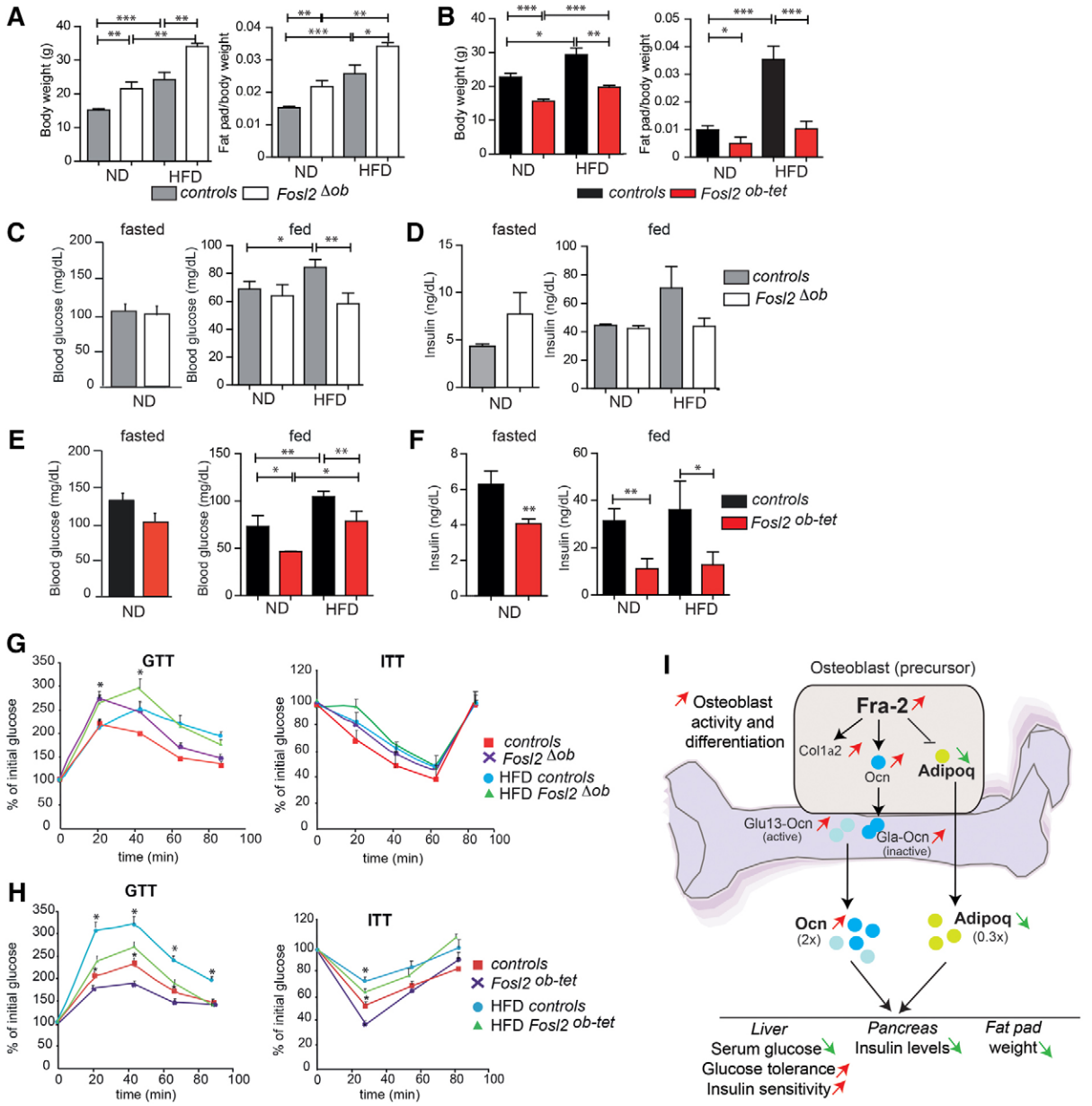

Fig. 4. Metabolic phenotypes of *Fosl2*$^{\Delta ob}$ and *Fosl2*$^{ob\text{-}tet}$ mice. (A,B) Weight of mice and fat pad/total weight from controls and *Fosl2*$^{\Delta ob}$ (A) or *Fosl2*$^{ob\text{-}tet}$ (B) mice under a ND or HFD for 6 weeks; error bars represent s.d. (n=6). (C,D) Serum glucose (C) and insulin (D) levels in controls and *Fosl2*$^{\Delta ob}$ mice following 6 weeks of a ND or HFD in fasted or fed conditions; error bars represent s.d. (n=6). (E,F) Serum glucose (E) and insulin (F) levels in *controls* and *Fosl2*$^{ob\text{-}tet}$ mice following 6 weeks of ND or HFD in fasted or fed conditions; error bars represent s.d. (n=6). (G,H) Glucose tolerance (GTT) and insulin tolerance (ITT) tests after 6 hours or 3 hours fasting from *Fosl2*$^{\Delta ob}$ (g) and *Fosl2*$^{ob\text{-}tet}$ (h) mice following 6 weeks of a ND or HFD (n=6 or 7). *P<0.05, **P<0.01, ***P<0.001. (I) Model depicting how Fra-2 expression in osteoblasts regulates glucose and insulin responses. In *Fosl2*$^{ob\text{-}tet}$ mice, osteoblast expression of Fra-2 leads to transcriptional repression of *Adipoq* and increased Ocn expression. The alteration of Ocn and Adipoq levels leads to a decrease in body weight as well as altered glucose and insulin levels and responses.

gluconeogenesis, regulation of fatty acid metabolism and modulation of Ca^{2+} signaling in skeletal muscle (Kadowaki et al., 2006). Adipoq self-associates into larger structures e.g. homotrimers (LMW), hexamers (MMW) or dodecamers (HMW), with the latter described as the bioactive form (Engl et al., 2007). In sera of *Fosl2*$^{ob\text{-}tet}$ mice, a decrease in LMW and MMW, and HMW Adipoq is associated with a decrease in insulin levels, and increased insulin sensitivity. Adipoq has been described as an adipokine produced mainly by adipocytes in fat tissue; surprisingly, its expression was unchanged in the fat pad of osteoblast-specific Fra-2 mutant mice. Importantly, Adipoq was expressed in osteoblasts and osteocytes, confirmed by Adipoq reporter mice (Eguchi et al., 2011). These findings support previous reports indicating that Adipoq and its receptors are expressed in bone-forming cells in humans (Berner et al., 2004) and in mice (Shinoda et al., 2006) as well as our microarray data on osteoblast cultures (M.A., unpublished data). We found that Adipoq expression is controlled by Fra-2 in a cell-autonomous manner in osteoblasts; Fra-2 directly represses the transcription of

Adipoq with JunD or c-Jun as dimer partners. The levels of Adipoq in the Fra-2 mutant mice are inversely correlated with the osteogenic potential of these cells *in vitro* and with bone mass *in vivo*. Studies *in vitro* and *in vivo* have yielded contradictory results regarding the effects of Adipoq on bone cell function. Adipoq has been shown to either stimulate or suppress osteogenesis *in vitro* (Lee et al., 2009; Shinoda et al., 2006; Williams et al., 2009) and the results from *in vivo* studies using Adipoq knockout or overexpressing mice are also conflicting (Ealey et al., 2008; Oshima et al., 2005; Shinoda et al., 2006; Williams et al., 2009). This indicates that Adipoq could additionally contribute to the bone phenotype by suppressing bone forming activity in osteoblasts in an autocrine fashion.

Our data suggest that Adipoq is a molecule linking bone physiology to systemic metabolism in an endocrine fashion, much like Ocn. Further experiments would be necessary to define its precise action given that the Fra-2 mutant mice described in this study show deregulation of at least two 'bone hormones', Adipoq and Ocn. Both forms of Ocn – the bioactive undercarboxylated Glu13 and the carboxylated Gla13-Ocn were induced by Fra-2. The Glu-Ocn controls insulin secretion and sensitivity (Ferron et al., 2010; Yoshizawa et al., 2009). Although Glu-Ocn has also been reported to induce Adipoq secretion by white adipocytes (Ferron et al., 2008; Lee and Karsenty, 2008; Lee et al., 2007), reduced circulating Adipoq was observed in $Fosl2^{ob\text{-}tet}$ mice despite increased Ocn. This suggests that Adipoq expression might exert its action independently of Ocn in Fra-2 mutant osteoblasts. Moreover, administration of exogenous Adipoq increased the circulating Adipoq to levels comparable to controls. Interestingly, under all conditions Ocn levels remained high in $Fosl2^{ob\text{-}tet}$ mice. Because the restoration of Adipoq levels through Ad-Adipoq in $Fosl2^{ob\text{-}tet}$ mice was sufficient to rescue glucose and insulin responses under a ND, we conclude that decreased Adipoq is partially responsible for the metabolic phenotype. The absence of complete rescue of insulin responses when $Fosl2^{ob\text{-}tet}$ mice were challenged with HFD might be due to the low Ad-Adipoq dose and/or to the timeline of the treatment.

Fra-2 has not yet been associated with a metabolic phenotype in humans, although it is possible that polymorphisms in Fra-2 exist. Fra-2 target genes, such as leptin, Adipoq and Ocn are associated with effects on glucose metabolism in mice and humans. Furthermore, increased Ocn levels in mice were associated with improved glucose handling and protection against the development of type 2 diabetes following diet-induced obesity (Ferron et al., 2012). The protection from diet-induced metabolic effects in $Fosl2^{ob\text{-}tet}$ mice challenged with a HFD allowed us to speculate that Fra-2 in osteoblasts protects against the adverse effects of obesity. These data add new evidence to the notion that osteoblasts are endocrine cells and that the skeleton is an endocrine organ. Therefore, modulating the activity of AP-1 transcription factors in osteoblasts might provide means for targeted therapies against metabolic diseases.

Materials and Methods

Mice

Osteoblast-specific Fra-2 deficient mice ($Fosl2^{\Delta ob}$) were generated by crossing *Fosl2 flox/flox* mice (Eferl et al., 2007) with mice carrying the *Osx-tTA-Cre* allele (Rodda and McMahon, 2006). The tetracycline (tet)-switchable *Fosl2* allele was introduced 3′ of the *col1a1* locus using a recombinase-mediated single-copy transgene integration strategy in embryonic stem cells (ESCs) (Beard et al., 2006). Southern blot analyses confirmed correct recombination in ESCs and correct germ-line transmission. Doxycycline-switchable expression of the FLAG-tagged mouse *Fosl2* cDNA sequence and the dsRed reporter were confirmed in ESCs and in mice with a tetracycline activator expressed from the *Rosa26* locus. Crossing mice with the tet-switchable *Fosl2* allele with Osx-tTA-Cre mice generated the osteoblast-specific $Fosl2^{ob\text{-}tet}$ mice. In the absence of doxycycline, these mice express Fra-2. Males were used for the metabolic studies. All mice were maintained on a mixed C57Bl6/129 background and littermates were used as controls.

All mice were bred and maintained without doxycycline to ensure Cre and *Fosl2* expression before birth and in adult. Genotyping was performed by PCR analyses of genomic DNA from tail biopsies. The generation of $Fosl2^{-/-}$ mice has been described previously (Bozec et al., 2008; Bozec et al., 2010; Eferl et al., 2007). Mutant mice expressing Td Tomato, a reporter for red fluorescent protein (RFP) under the control of the *Adipoq* promoter were obtained by crossing the lox-STOP-lox Td Tomato mice with Adipoq-Cre mice (Eguchi et al., 2011). For HFD experiments, six-week-old mice were challenged with a high fat diet (D12331 from Research Diet NC) for six weeks. All mouse experiments were performed in accordance with local and institutional regulations.

Metabolic studies

For the GTT assay, glucose (2 g/kg of body weight) was injected intraperitoneally (i.p.) after 6 hours of fasting, and blood glucose was monitored using blood glucose strips and the accu-check glucometer (Roche) at indicated times. For the ITT assay, insulin (0.55 U/kg of body weight) was injected i.p. after 3 hours of fasting and blood glucose levels were measured at indicated time.

Insulin-induced pAKT responses

Mice were fasted overnight and injected i.p. with vehicle or insulin (1 U/kg of body weight). At 15 minutes after injection, mice were killed and proteins were isolated from fat, liver and muscle. Western blotting for pAKT (Cell Signaling) and AKT (Cell Signaling) was performed.

Laboratory measurements

Blood was collected by heart puncture. Serum levels of insulin (Mercodia), leptin (R&D Systems), resistin (R&D system), total Adipoq and HMW Adipoq (Alpco and Abcam) were quantified by ELISA. Protein from pancreas and bone were isolated, and insulin and protein levels were quantified using insulin ELISA (Mercodia) and the Bradford kit (PIERCE), respectively.

Osteocalcin measurement

Sera from mice were added to hydroxyapatite (HA) to achieve a final concentration of 25 mg/ml. After 60 minutes HA beads were pelleted by centrifugation and HA-unbound osteocalcin was used. The osteocalcin level in supernatant and initial samples were measured by ELISA (Demetitec diagnostic).

Histological analyses

Bones were fixed in 10% neutral formalin and decalcified. Bone were embedded in paraffin and sectioned at 5 µm. Immunohistochemical staining for Fra-2 (Abcam), RFP (molecular probes), Adipoq (Abcam and Santa Cruz Biotechnology), TRAP (Sigma) and Ocn (Enzo laboratories) were performed on deparaffinized sections using the LSAB or Envision detection kit (Dako). For immunofluorescence on paraffin sections, secondary antibodies used were conjugated to Texas Red (The Jackson Laboratory) and counterstainings were performed with DAPI. Double immunofluorescence was performed on paraffin sections using RFP and Ocn antibodies and secondary antibodies conjugated to Texas Red or FITC (Abcam) in a simulatenous protocol (Abcam). For histomorphometrical analysis, undecalcified lumbar spines were embedded in methylmethacrylate and 5-µm sections were cut along the sagittal plane. Sections were stained with Toluidine Blue, and modified von Kossa/van Gieson. Quantitative histomorphometry was performed on Toluidine-Blue-stained sections according to standard protocols (Parfitt et al., 1987) using the Osteomeasure histomorphometry system (Osteometrix). Experiments were performed in a blinded fashion.

Osteoblast, adipocyte and osteoclast cultures

Calvariae were sequentially digested for 30 minutes in modified Eagle's medium type α (α-MEM) containing 0.1% collagenase and 0.2% dispase. Cells isolated in fractions 2–3 were combined as an osteoblastic cell population, expanded for 2 days in α-MEM with 10% fetal calf serum (FCS) and plated at a density of 5×10^5 cells/well. Medium was supplemented with 10 mM β-glycerophosphate and 50 µg/ml ascorbic acid for osteoblast cultures or with 1 mM dexamethasone (Sigma-Aldrich), and 10 mg/ml insulin (Sigma-Aldrich) for adipocyte cultures. After 2 weeks of culture, RNAs were extracted from osteoblast or adipocyte cultures. To control cell differentiation, Alizarin Red (Sigma-Aldrich) and Oil Red O (Sigma-Aldrich) staining were performed for osteoblast and adipocyte cultures.

Bone marrow cells were isolated from six-week-old mice, put into suspension overnight and cultured in 24 wells (5×10^5 cells/well) for 2–7 days with macrophage colony-stimulating factor (20 ng/ml; R&D) and Rankl (5 ng/ml; R&D); TRAP straining (Sigma-Aldrich) was then performed.

RNA isolation, reverse transcription

Total RNA was isolated with the TRIzol protocol (Invitrogen). For bone samples whole long-bones, including marrow, was extracted. cDNA synthesis was performed

using 2 μg RNA with the Ready-To-GoTM You-Prime It First-Strand-Beads and random primers (Amersham Biosciences) according to the manufacturer's protocols.

Real-time PCR analyses

qPCR reactions were performed using SYBR Green (Molecular Probes) on MasterCycler ep Realplex (Eppendorf). Primers for genes analyses used for real-time PCR are available upon request. The comparative CT method was used to quantify the amplified fragments. RNA expression levels were normalized to those of actin. Results are shown as mean± s.d. of gene expression relative to actin.

Western blotting

Whole long bone, pancreas, fat pad and culture cells extracts were prepared with cell RIPA lysis buffer and western blots were performed with the antibodies against the following proteins: Fra-2 (Invitrogen), Flag (Sigma), Adipoq (Abcam and Santa-Cruz) and for normalizing, actin (Sigma).

ChIP

ChIP was performed according to standard protocols with antibodies against Fra-2, Fra-1, FosB, c-Fos, JunB, JunD, c-Jun, ATF4 (Santa Cruz Biotechnology), K4 (Upstate) and K27 (kind gift from Thomas Jenuwein). The specific binding of Fra-2 antibody was verified in parallel using a corresponding pair of wt and ko osteoblasts in 3 independent experiments.

The promoter–reporter vectors of adiponectin promoter were generated using pGL4.23[luc2/minP] vector following the kit instructions (Promega). 6×10^4 HEK293 cells/well were plated in 24-well dishes. 1.5 μg of the luciferase reporter construct, 0.2 μg of the *Renilla* internal control (pHRG-tk; Promega) and 0.2–1 μg of each AP-1 expression vector were co-transfected in triplicate using Lipofectamine (Invitrogen). cJun–Fra-2 forced dimer constructs were generated as previously described (Bakiri et al., 2002). Luciferase activity was quantified using the Dual Luciferase kit (Promega).

Statistical analysis

All experiments were repeated at least three times and performed in triplicate. Statistical analysis was performed using the two-tailed non-parametric Student's *t*-test. The significance levels are: $*P<0.05$, $**P<0.01$ and $***P<0.001$. Data are shown as means±s.d.

Acknowledgements

We are very grateful to Jean-Pierre David, Rama Khokha, Michele Petrucelli, Francesco Real, Romeo Ricci, Mercedes Rincon, Özge Uluckan and Juan Guinea-Viniegra for critically reading the manuscript and Lionel Gresh for help in generating the *Fosl2*$^{ob\text{-}tet}$ transgenic line. We also thank Thomas Jenuwein for providing the methyl histone antibodies.

Author contributions

A.B., M.J., P.C.-L. and T.S. collected the data; E.D.R. provided Adipoq Cre mice; M.A. and G.S. read the paper and provided valuable comments, A.B., L.B. and E.F.W. designed the study and wrote the manuscript.

Funding

This work was supported by the German Research Foundation (DFG) [grant number B38111-1 to A.B.]; an European Research Council Advanced grant [grant number ERC FCK/2008/37 to E.F.W.]; and the Banco Bilbao Vizcaya Argentaria Foundation (F-BBVA).

Supplementary material available online at
http://jcs.biologists.org/lookup/suppl/doi:10.1242/jcs.134510/-/DC1

References

Bakiri, L., Matsuo, K., Wisniewska, M., Wagner, E. F. and Yaniv, M. (2002). Promoter specificity and biological activity of tethered AP-1 dimers. *Mol. Cell. Biol.* **22**, 4952-4964.

Beard, C., Hochedlinger, K., Plath, K., Wutz, A. and Jaenisch, R. (2006). Efficient method to generate single-copy transgenic mice by site-specific integration in embryonic stem cells. *Genesis* **44**, 23-28.

Berner, H. S., Lyngstadaas, S. P., Spahr, A., Monjo, M., Thommesen, L., Drevon, C. A., Syversen, U. and Reseland, J. E. (2004). Adiponectin and its receptors are expressed in bone-forming cells. *Bone* **35**, 842-849.

Bozec, A., Bakiri, L., Hoebertz, A., Eferl, R., Schilling, A. F., Komnenovic, V., Scheuch, H., Priemel, M., Stewart, C. L., Amling, M. et al. (2008). Osteoclast size is controlled by Fra-2 through LIF/LIF-receptor signalling and hypoxia. *Nature* **454**, 221-225.

Bozec, A., Bakiri, L., Jimenez, M., Schinke, T., Amling, M. and Wagner, E. F. (2010). Fra-2/AP-1 controls bone formation by regulating osteoblast differentiation and collagen production. *J. Cell Biol.* **190**, 1093-1106.

Ealey, K. N., Kaludjerovic, J., Archer, M. C. and Ward, W. E. (2008). Adiponectin is a negative regulator of bone mineral and bone strength in growing mice. *Exp. Biol. Med.* **233**, 1546-1553.

Eferl, R., Hoebertz, A., Schilling, A. F., Rath, M., Karreth, F., Kenner, L., Amling, M. and Wagner, E. F. (2004). The Fos-related antigen Fra-1 is an activator of bone matrix formation. *EMBO J.* **23**, 2789-2799.

Eferl, R., Zenz, R., Theussl, H. C. and Wagner, E. F. (2007). Simultaneous generation of fra-2 conditional and fra-2 knock-out mice. *Genesis* **45**, 447-451.

Eferl, R., Hasselblatt, P., Rath, M., Popper, H., Zenz, R., Komnenovic, V., Idarraga, M. H., Kenner, L. and Wagner, E. F. (2008). Development of pulmonary fibrosis through a pathway involving the transcription factor Fra-2/AP-1. *Proc. Natl. Acad. Sci. USA* **105**, 10525-10530.

Eguchi, J., Wang, X., Yu, S., Kershaw, E. E., Chiu, P. C., Dushay, J., Estall, J. L., Klein, U., Maratos-Flier, E. and Rosen, E. D. (2011). Transcriptional control of adipose lipid handling by IRF4. *Cell Metab.* **13**, 249-259.

Engl, J., Bobbert, T., Ciardi, C., Laimer, M., Tatarczyk, T., Kaser, S., Weiss, H., Molnar, C., Tilg, H., Patsch, J. R. et al. (2007). Effects of pronounced weight loss on adiponectin oligomer composition and metabolic parameters. *Obesity* **15**, 1172-1178.

Ferron, M., Hinoi, E., Karsenty, G. and Ducy, P. (2008). Osteocalcin differentially regulates beta cell and adipocyte gene expression and affects the development of metabolic diseases in wild-type mice. *Proc. Natl. Acad. Sci. USA* **105**, 5266-5270.

Ferron, M., Wei, J., Yoshizawa, T., Del Fattore, A., DePinho, R. A., Teti, A., Ducy, P. and Karsenty, G. (2010). Insulin signaling in osteoblasts integrates bone remodeling and energy metabolism. *Cell* **142**, 296-308.

Ferron, M., McKee, M. D., Levine, R. L., Ducy, P. and Karsenty, G. (2012). Intermittent injections of osteocalcin improve glucose metabolism and prevent type 2 diabetes in mice. *Bone* **50**, 568-575.

Grigoriadis, A. E., Schellander, K., Wang, Z. Q. and Wagner, E. F. (1993). Osteoblasts are target cells for transformation in c-fos transgenic mice. *J. Cell Biol.* **122**, 685-701.

Kadowaki, T., Yamauchi, T., Kubota, N., Hara, K., Ueki, K. and Tobe, K. (2006). Adiponectin and adiponectin receptors in insulin resistance, diabetes, and the metabolic syndrome. *J. Clin. Invest.* **116**, 1784-1792.

Karreth, F., Hoebertz, A., Scheuch, H., Eferl, R. and Wagner, E. F. (2004). The AP1 transcription factor Fra2 is required for efficient cartilage development. *Development* **131**, 5717-5725.

Karsenty, G. and Ferron, M. (2012). The contribution of bone to whole-organism physiology. *Nature* **481**, 314-320.

Kawai, M., Devlin, M. J. and Rosen, C. J. (2009). Fat targets for skeletal health. *Nat. Rev. Rheumatology* **5**, 365-372.

Kveiborg, M., Chiusaroli, R., Sims, N. A., Wu, M., Sabatakos, G., Horne, W. C. and Baron, R. (2002). The increased bone mass in deltaFosB transgenic mice is independent of circulating leptin levels. *Endocrinology* **143**, 4304-4309.

Lee, N. K. and Karsenty, G. (2008). Reciprocal regulation of bone and energy metabolism. *Trends Endocrinol.* **Metab.19**, 161-166.

Lee, N. K., Sowa, H., Hinoi, E., Ferron, M., Ahn, J. D., Confavreux, C., Dacquin, R., Mee, P. J., McKee, M. D., Jung, D. Y. et al. (2007). Endocrine regulation of energy metabolism by the skeleton. *Cell* **130**, 456-469.

Lee, H. W., Kim, S. Y., Kim, A. Y., Lee, E. J., Choi, J. Y. and Kim, J. B. (2009). Adiponectin stimulates osteoblast differentiation through induction of COX2 in mesenchymal progenitor cells. *Stem Cells* **27**, 2254-2262.

Lefterova, M. I. and Lazar, M. A. (2009). New developments in adipogenesis. *Trends Endocrinol. Metab.* **20**, 107-114.

Luther, J., Driessler, F., Megges, M., Hess, A., Herbort, B., Mandic, V., Zaiss, M. M., Reichardt, A., Zech, C., Tuckermann, J. P. et al. (2011). Elevated Fra-1 expression causes severe lipodystrophy. *J. Cell Sci.* **124**, 1465-1476.

Oshima, K., Nampei, A., Matsuda, M., Iwaki, M., Fukuhara, A., Hashimoto, J., Yoshikawa, H. and Shimomura, I. (2005). Adiponectin increases bone mass by suppressing osteoclast and activating osteoblast. *Biochem. Biophys. Res. Commun.* **331**, 520-526.

Oury, F., Sumara, G., Sumara, O., Ferron, M., Chang, H., Smith, C. E., Hermo, L., Suarez, S., Roth, B. L., Ducy, P. et al. (2011). Endocrine regulation of male fertility by the skeleton. *Cell* **144**, 796-809.

Parfitt, A. M., Drezner, M. K., Glorieux, F. H., Kanis, J. A., Malluche, H., Meunier, P. J., Ott, S. M., Recker, R. R.; Report of the ASBMR Histomorphometry Nomenclature Committee (1987). Bone histomorphometry: standardization of nomenclature, symbols, and units. *J. Bone Miner. Res.* **2**, 595-610.

Rached, M. T., Kode, A., Xu, L., Yoshikawa, Y., Paik, J. H., Depinho, R. A. and Kousteni, S. (2010). FoxO1 is a positive regulator of bone formation by favoring protein synthesis and resistance to oxidative stress in osteoblasts. *Cell Metab.* **11**, 147-160.

Rodda, S. J. and McMahon, A. P. (2006). Distinct roles for Hedgehog and canonical Wnt signaling in specification, differentiation and maintenance of osteoblast progenitors. *Development* **133**, 3231-3244.

Shetty, S., Kusminski, C. M. and Scherer, P. E. (2009). Adiponectin in health and disease: evaluation of adiponectin-targeted drug development strategies. *Trends Pharmacol. Sci.* **30**, 234-239.

Shinoda, Y., Yamaguchi, M., Ogata, N., Akune, T., Kubota, N., Yamauchi, T., Terauchi, Y., Kadowaki, T., Takeuchi, Y., Fukumoto, S. et al. (2006). Regulation

of bone formation by adiponectin through autocrine/paracrine and endocrine pathways. *J. Cell. Biochem.* **99**, 196-208.

Takeda, S., Elefteriou, F., Levasseur, R., Liu, X., Zhao, L., Parker, K. L., Armstrong, D., Ducy, P. and Karsenty, G. (2002). Leptin regulates bone formation via the sympathetic nervous system. *Cell* **111**, 305-317.

Tilg, H. and Moschen, A. R. (2006). Adipocytokines: mediators linking adipose tissue, inflammation and immunity. *Nat. Rev. Immunol.* **6**, 772-783.

Wagner, E. F. and Eferl, R. (2005). Fos/AP-1 proteins in bone and the immune system. *Immunol. Rev.* **208**, 126-140.

Williams, G. A., Wang, Y., Callon, K. E., Watson, M., Lin, J. M., Lam, J. B., Costa, J. L., Orpe, A., Broom, N., Naot, D. et al. (2009). In vitro and in vivo effects of adiponectin on bone. *Endocrinology* **150**, 3603-3610.

Wrann, C. D., Eguchi, J., Bozec, A., Xu, Z., Mikkelsen, T., Gimble, J., Nave, H., Wagner, E. F., Ong, S. E. and Rosen, E. D. (2012). FOSL2 promotes leptin gene expression in human and mouse adipocytes. *J. Clin. Invest.* **122**, 1010-1021.

Yang, X. and Karsenty, G. (2004). ATF4, the osteoblast accumulation of which is determined post-translationally, can induce osteoblast-specific gene expression in non-osteoblastic cells. *J. Biol. Chem.* **279**, 47109-47114.

Yang, X., Matsuda, K., Bialek, P., Jacquot, S., Masuoka, H. C., Schinke, T., Li, L., Brancorsini, S., Sassone-Corsi, P., Townes, T. M. et al. (2004). ATF4 is a substrate of RSK2 and an essential regulator of osteoblast biology; implication for Coffin-Lowry Syndrome. *Cell* **117**, 387-398.

Yoshizawa, T., Hinoi, E., Jung, D. Y., Kajimura, D., Ferron, M., Seo, J., Graff, J. M., Kim, J. K. and Karsenty, G. (2009). The transcription factor ATF4 regulates glucose metabolism in mice through its expression in osteoblasts. *J. Clin. Invest.* **119**, 2807-2817.

Zhao, L. J., Jiang, H., Papasian, C. J., Maulik, D., Drees, B., Hamilton, J. and Deng, H. W. (2008). Correlation of obesity and osteoporosis: effect of fat mass on the determination of osteoporosis. *J. Bone Miner. Res.* **23**, 17-29.

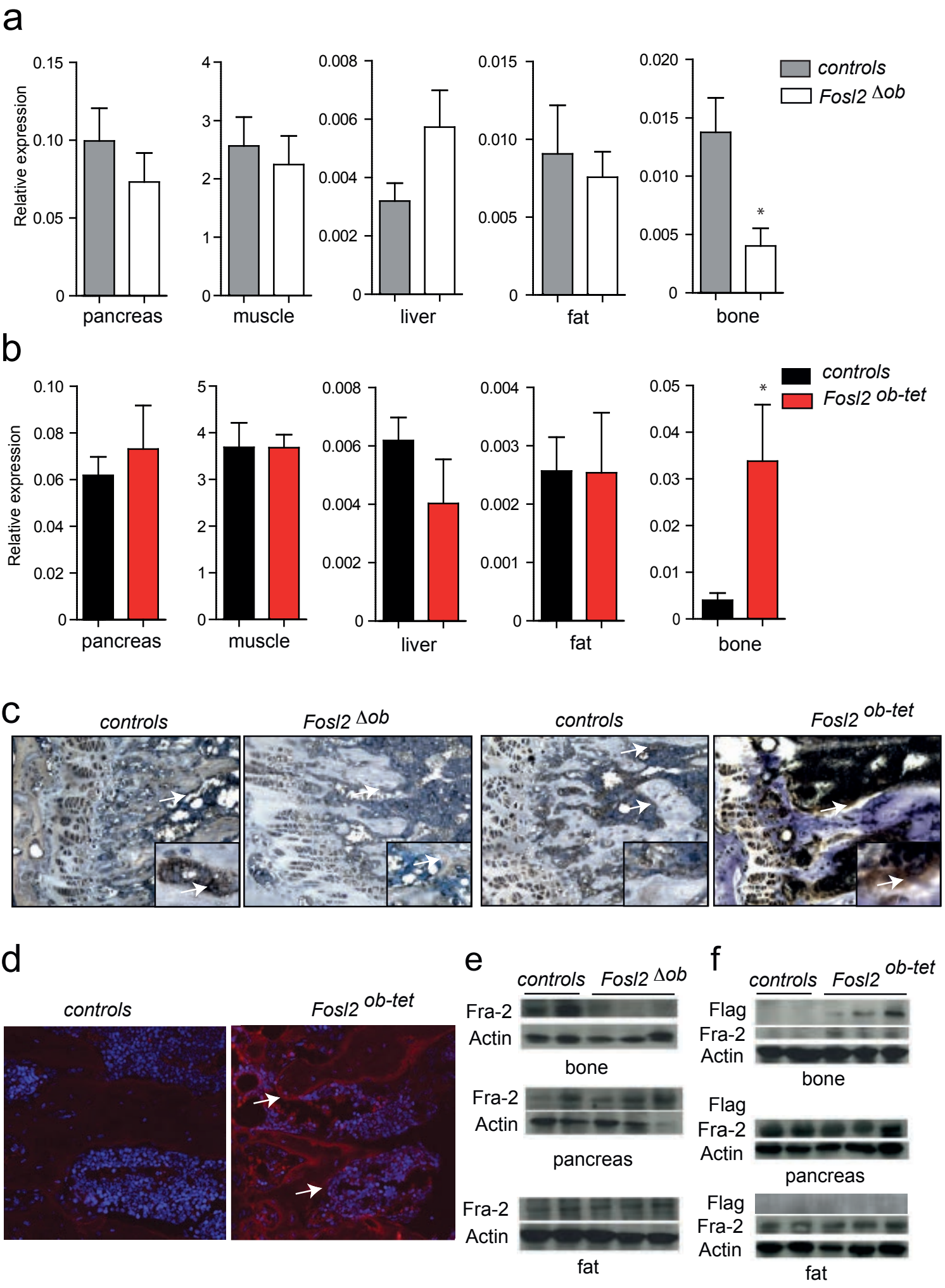
a
Relative expression
0.15
0.10
0.05
0
pancreas
4
3
2
1
0
muscle
0.008
0.006
0.004
0.002
0
liver
0.015
0.010
0.005
0
fat
0.020
0.015
0.010
0.005
0
*
bone
controls
Fosl2 Δob
b
Relative expression
0.10
0.08
0.06
0.04
0.02
0
pancreas
5
4
3
2
1
0
muscle
0.008
0.006
0.004
0.002
0
liver
0.004
0.003
0.002
0.001
0
fat
0.05
0.04
0.03
0.02
0.01
0
*
bone
controls
Fosl2 ob-tet
c
controls
Fosl2 Δob
controls
Fosl2 ob-tet
d
controls
Fosl2 ob-tet
e
controls
Fosl2 Δob
Fra-2
Actin
bone
Fra-2
Actin
pancreas
Fra-2
Actin
fat
f
controls
Fosl2 ob-tet
Flag
Fra-2
Actin
bone
Flag
Fra-2
Actin
pancreas
Flag
Fra-2
Actin
fat

Bozec *et al.* Sup Fig 2

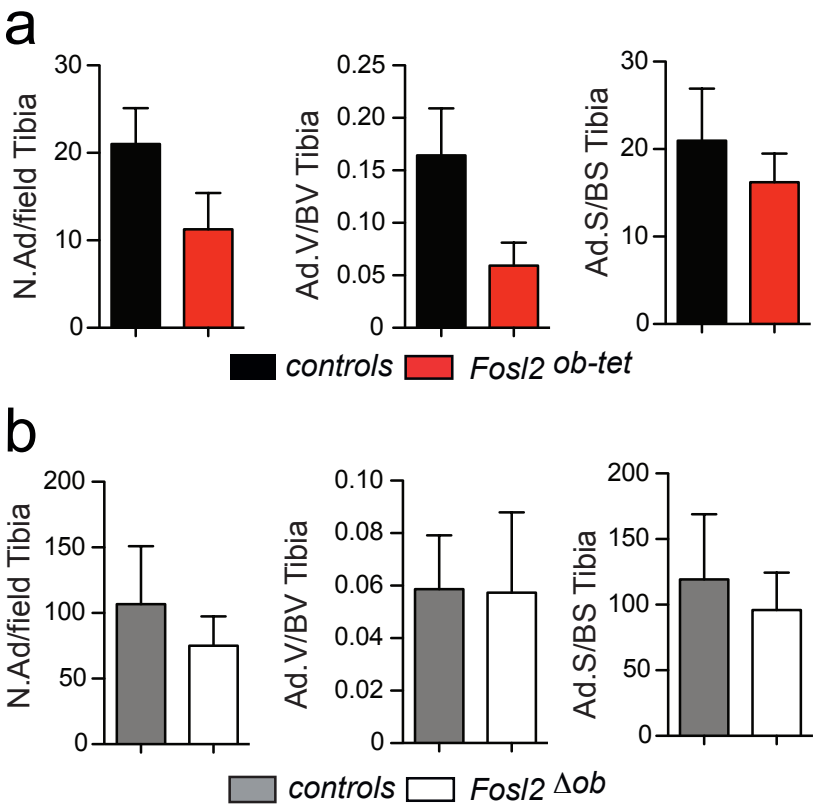

Bozec *et al.* Sup Fig. 3

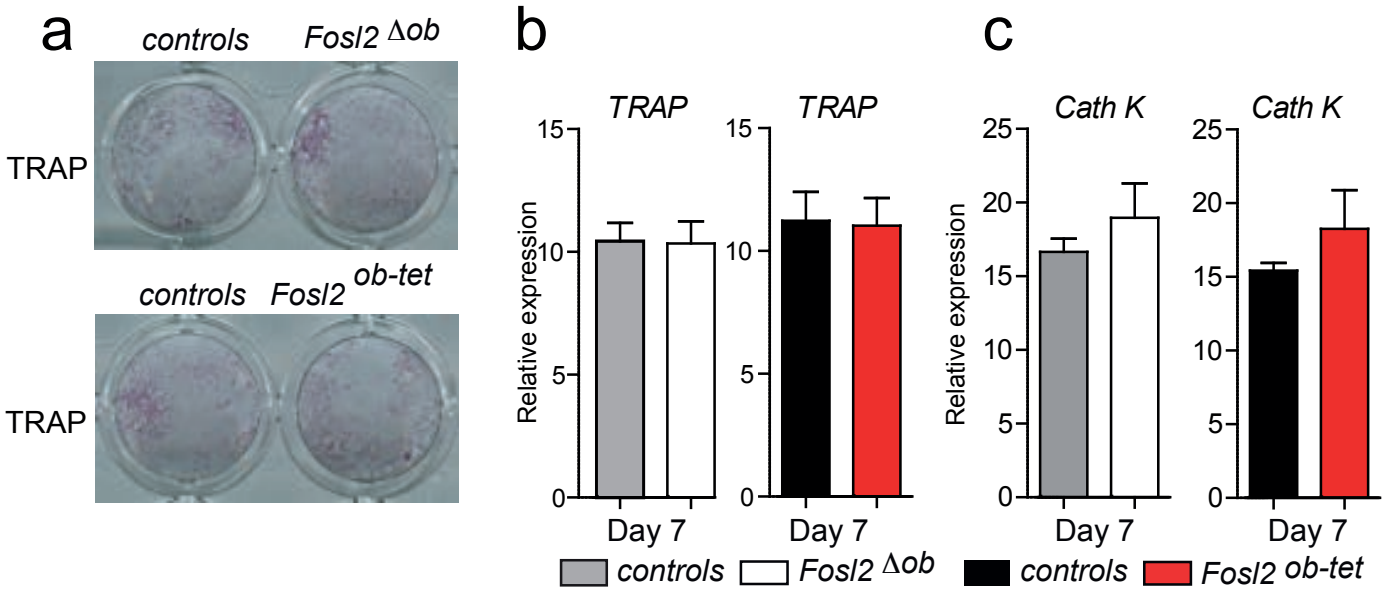

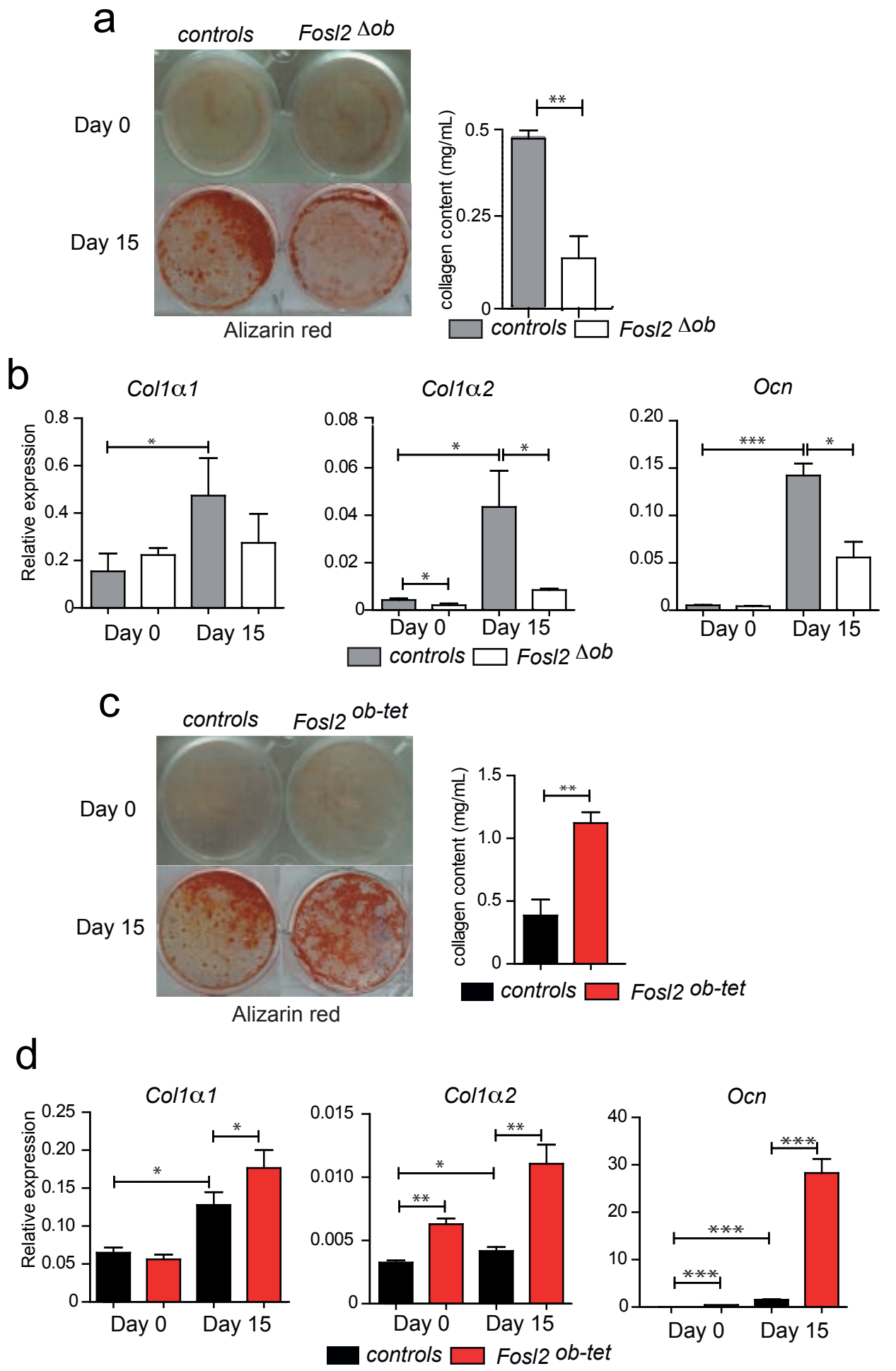
a
controls
Fosl2 Δob
Day 0
Day 15
Alizarin red
collagen content (mg/mL)
0.5
0.25
0
**
controls
Fosl2 Δob
b
Col1α1
Col1α2
Ocn
Relative expression
0.8
0.6
0.4
0.2
0
0.08
0.06
0.04
0.02
0.20
0.15
0.10
0.05
*
***
Day 0
Day 15
controls
Fosl2 Δob
c
controls
Fosl2 ob-tet
Day 0
Day 15
Alizarin red
collagen content (mg/mL)
1.5
1.0
0.5
0
**
controls
Fosl2 ob-tet
d
Col1α1
Col1α2
Ocn
Relative expression
0.25
0.20
0.15
0.10
0.05
0
0.015
0.010
0.005
40
30
20
10
*
**
***
Day 0
Day 15
controls
Fosl2 ob-tet

Bozec *et al.* Sup Fig. 5

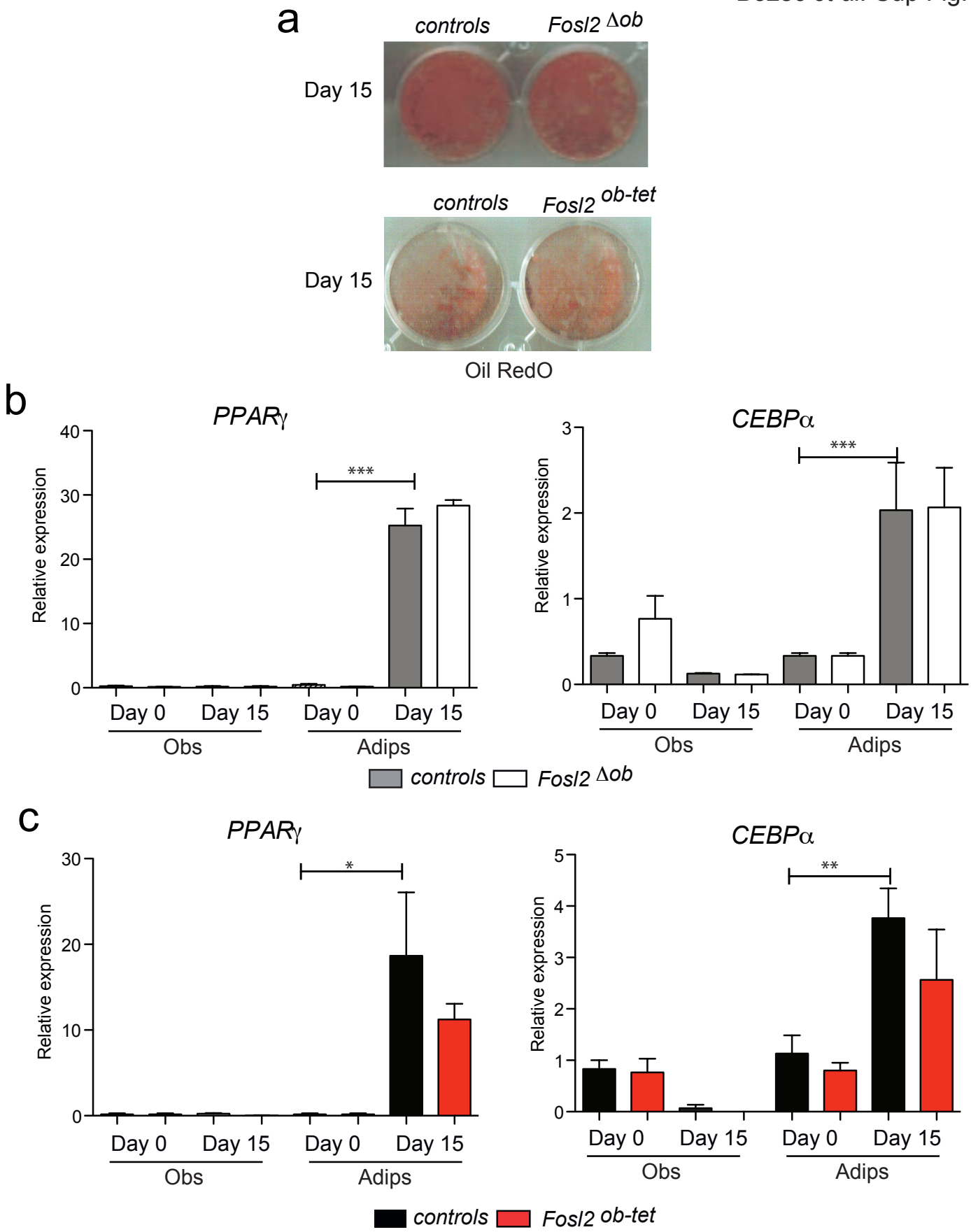

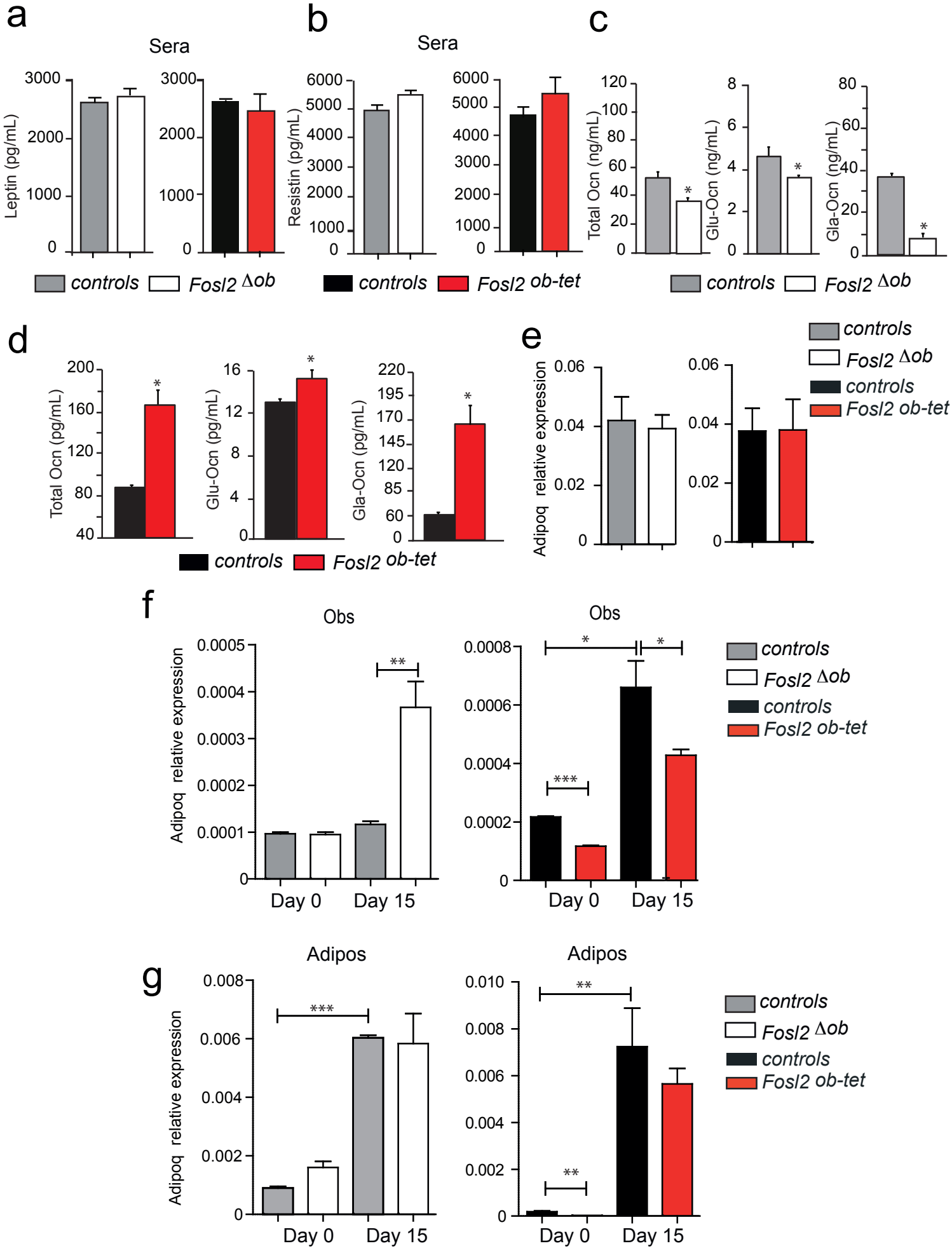
a
Sera
Leptin (pg/mL)
3000
2000
1000
0
controls
Fosl2 Δob
b
Sera
Resistin (pg/mL)
6000
5000
4000
3000
2000
1000
0
controls
Fosl2 ob-tet
c
Total Ocn (ng/mL)
Glu-Ocn (ng/mL)
Gla-Ocn (ng/mL)
controls
Fosl2 Δob
d
Total Ocn (pg/mL)
Glu-Ocn (pg/mL)
Gla-Ocn (pg/mL)
controls
Fosl2 ob-tet
e
Adipoq relative expression
controls
Fosl2 Δob
controls
Fosl2 ob-tet
f
Obs
Adipoq relative expression
Day 0
Day 15
g
Adipos
Adipoq relative expression
Day 0
Day 15

Bozec *et al.* Sup Fig. 7

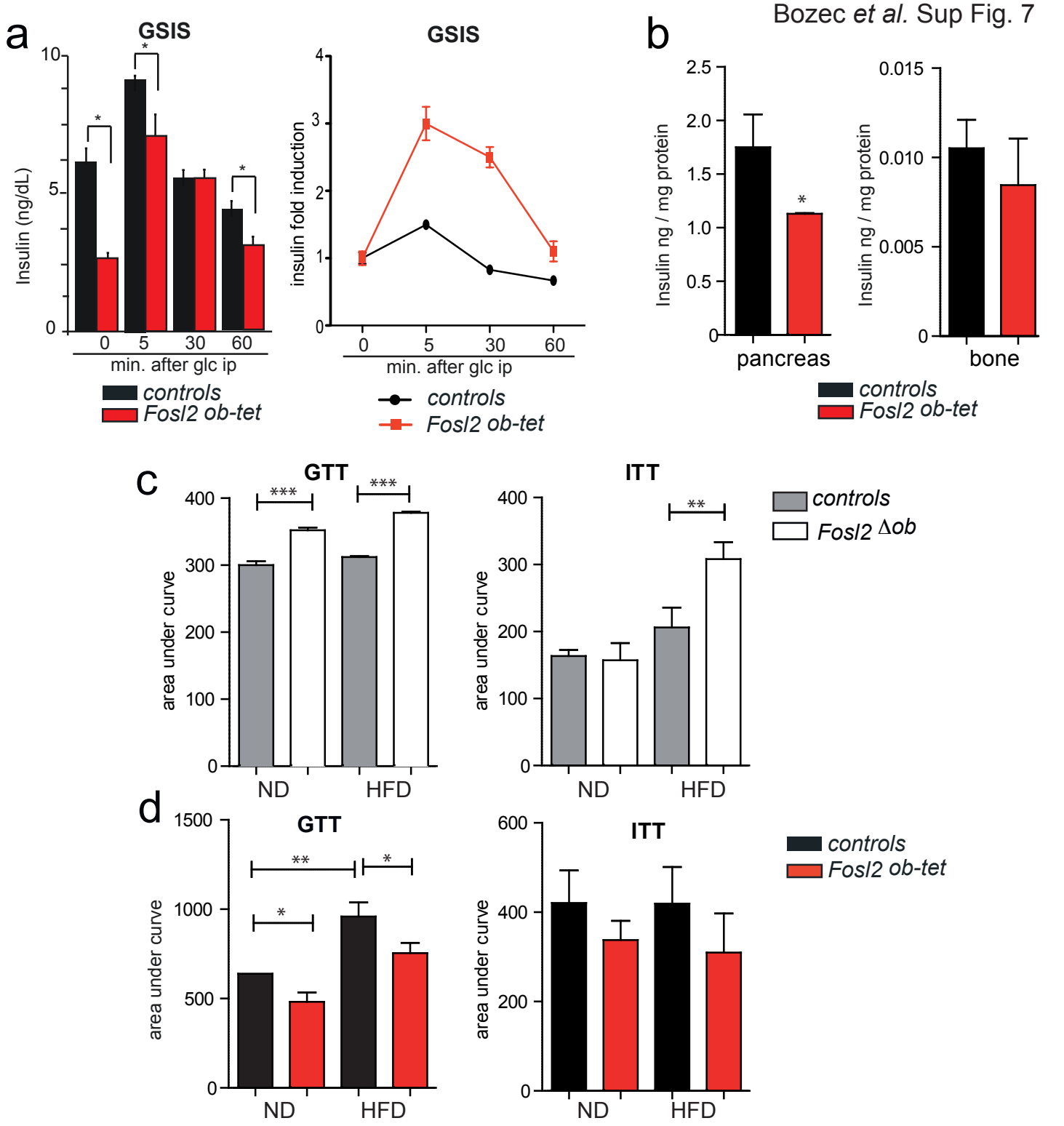

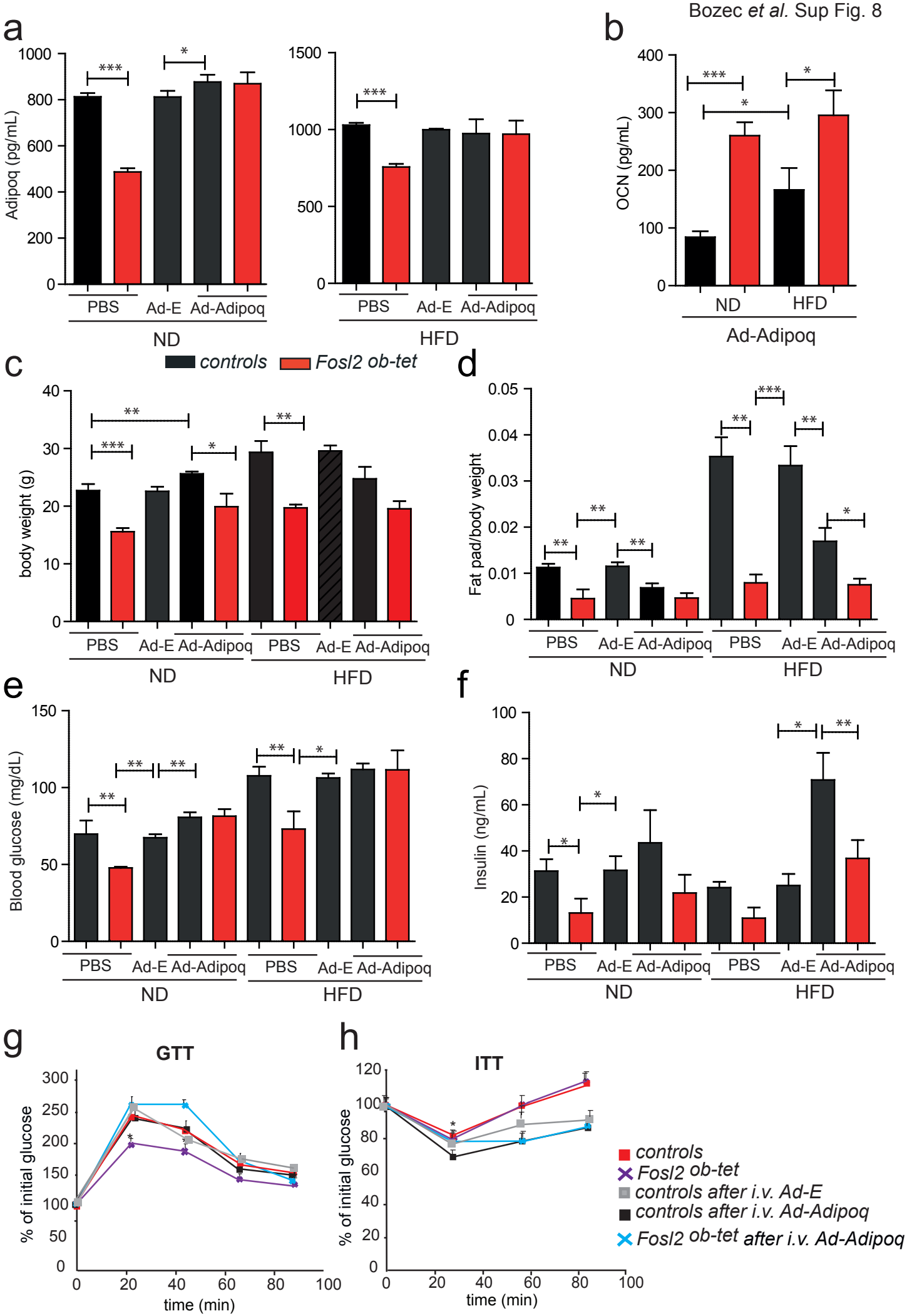
a
Adipoq (pg/mL)
PBS
Ad-E
Ad-Adipoq
ND
HFD
b
OCN (pg/mL)
ND
HFD
Ad-Adipoq
c
controls
Fosl2 ob-tet
body weight (g)
d
Fat pad/body weight
e
Blood glucose (mg/dL)
f
Insulin (ng/mL)
g
GTT
% of initial glucose
time (min)
h
ITT
controls
Fosl2 ob-tet
controls after i.v. Ad-E
controls after i.v. Ad-Adipoq
Fosl2 ob-tet after i.v. Ad-Adipoq

Fig. S1. Fra-2 expression in *Fosl2* $^{\Delta ob}$ and *Fosl2* $^{ob\text{-}tet}$ mice. a, b: qPCR analyses of Fra-2 in pancreas, muscle, liver, fat and bone from *Fosl2* $^{\Delta ob}$ (a) and *Fosl2*$^{ob\text{-}tet}$ (b) mice at 6 weeks of age; bars represent mean values ± SD (n=6). c: Immuno-histochemical (IHC) analyses of Fra-2 in *Fosl2* $^{\Delta ob}$ and *Fosl2* $^{ob\text{-}tet}$ long bones at 2 months of age; magnification 20x. Inserts: 40x. White arrows indicate osteoblasts. d: Immuno-fluorescence analyses of Fra-2 in *Fosl2* $^{ob\text{-}tet}$ long bones at 2 months of age; magnification 20x. White arrows indicate osteoblasts. e: Western blot analyses of Fra-2 in bone, pancreas and fat pad from controls and *Fosl2* $^{\Delta ob}$ mice at 6 weeks of age (n=2/3); actin was used as loading control. f: Western blot analyses of Flag and Fra-2 in bone, pancreas and fat pad from *controls* and *Fosl2*$^{ob\text{-}tet}$ mice at 6 weeks of age (n=2/3); actin was used as loading control. Statistical analyses: *P<0.05, **P<0.01, ***P<0.001.

Fig. S2. *In vivo* adipocyte phenotypes in osteoblast-specific Fra-2 mutant mice. a, b: Quantification of number of adipocytes per field Tibia (N.Ad/field Tibia), adipocyte volume per bone volume (Ad.V/BV Tibia) and adipocyte surface per bone surface (Ad.S/BS Tibia) in *Fosl2* $^{\Delta ob}$ (a) and *Fosl2* $^{ob\text{-}tet}$ (b) mice at 2 months of age (n=8).

Fig. S3. *In vitro* analyses of osteoclasts from osteoblast-specific Fra-2 mutant mice. a: TRAP staining in *Fosl2* $^{\Delta ob}$ and *Fosl2* $^{ob\text{-}tet}$ osteoclasts during differentiation at day 7 after addition of M-CSF and Rankl (n=3). b, c: qPCR analyses of *TRAP* (b) and *CathK* (c) in *Fosl2* $^{\Delta ob}$ and *Fosl2* $^{ob\text{-}tet}$ osteoclasts during differentiation at day 7 after addition of M-CSF and Rankl (n=3).

Fig. S4. *In vitro* analyses of osteoblasts from osteoblast-specific Fra-2 mutant mice. a: Alizarin red staining and collagen content of mineralized osteoblasts derived from calvariae of *Fosl2* $^{\Delta ob}$ mice at day 0 and 15 of *in vitro* differentiation (n=5). b: qPCR analyses of *col1α1, Col1α 2* and *Ocn* in osteoblasts from *Fosl2* $^{\Delta ob}$ cultures at day 0 and 15 of *in vitro* differentiation; error bars represent SD (n=6) c: Alizarin red staining and collagen content of mineralized osteoblasts derived from calvariae of *Fosl2* $^{ob\text{-}tet}$ mice at day 0 and 15 of *in vitro* differentiation (n=5). d: qPCR analyses of *col1α1, Col1α 2* and *Ocn* in osteoblasts from *Fosl2* $^{ob\text{-}tet}$ cultures at day 0 and 15 of *in vitro* differentiation; error bars represent SD (n=6). Statistical analyses: *P<0.05, **P<0.01, ***P<0.001.

Fig. S5. *In vitro* analyses of adipocytes from osteoblast-specific Fra-2 mutant mice. a: Oil RedO staining of adipocytes derived from calvariae of *Fosl2* $^{\Delta ob}$ and *Fosl2* $^{ob\text{-}tet}$ at day 15 of *in vitro* differentiation (n=3). b, c: qPCR analyses of *PPARγ* and *CEBPα* in osteoblasts and adipocytes from *Fosl2* $^{\Delta ob}$ (b) and *Fosl2* $^{ob\text{-}tet}$ (c) cultures at day 0 and 15 of *in vitro* differentiation; error bars represent SD (n=6). Statistical analyses: *P<0.05, **P<0.01, ***P<0.001

Fig. S6. Adiponectin expression in Fra-2 mutant mice. a, b: Leptin (a) and Resistin (b) levels in sera from controls and *Fosl2* $^{\Delta ob}$ or *Fosl2* $^{ob\text{-}tet}$ mice at 3 months of age; error bars represent SD (n=4/6). c, d: Total, Glu and Gla Ocn levels in sera from controls, *Fosl2* $^{\Delta ob}$ (c) and *Fosl2* $^{ob\text{-}tet}$ (d) mice (n=10). e: qPCR analyses of *Adipoq* in fat from *Fosl2* $^{\Delta ob}$ or *Fosl2* $^{ob\text{-}tet}$ mice at 3 months of age; error bars represent SD (n=6). f, g: qPCR analyses of *Adipoq* in osteoblasts (f) and adipocytes (g) from *Fosl2* $^{\Delta ob}$ and *Fosl2* $^{ob\text{-}tet}$ cultures at day 0 and 15 of *in vitro* differentiation; error bars represent SD (n=5). Statistical analyses: *P<0.05, **P<0.01, ***P<0.001.

Fig. S7. Metabolic phenotype of Fra-2 mutant mice. a: Glucose-stimulated insulin secretion (GSIS) graph and curve measured by insulin fold induction where time 0=1 in 3 months old *controls* and *Fosl2* $^{ob\text{-}tet}$ mice (n=6). b: Insulin content per mg protein of pancreas or bone from 3 months old *Fosl2* $^{ob\text{-}tet}$ mice; error bars represent SD (n=3). c, d: Area under curve analyses of the GTT and ITT tests after 6h or 3h fasting from *Fosl2* $^{\Delta ob}$ (c) and *Fosl2* $^{ob\text{-}tet}$ (d) mice following 6 weeks of ND or HFD; error bars represent SD (n=6/7). e-g: Western blot analyses of p-AKT and AKT in fat (e), liver (f) and muscle (g) from controls and *Fosl2* $^{\Delta ob}$ (left panel) or *Fosl2* $^{ob\text{-}tet}$ (right panel) mice 15 min after vehicle or insulin injection (n=4). Statistical analyses: *P<0.05, **P<0.01, ***P<0.001

Fig. S8. Injection of Adeno-Adipoq into *Fosl2* $^{ob\text{-}tet}$ mice partially rescues the metabolic phenotype. a: Adipoq levels in sera from *controls* and *Fosl2* $^{ob\text{-}tet}$ mice, under ND or HFD for 6 weeks, 12 days after i.v. injection of PBS (Co), Adeno-Empty (Ad-E) or Adeno-Adipoq (Ad-Adipoq); error bars represent SD. (n=6/8). b: Total Ocn levels in sera from *controls* and *Fosl2* $^{ob\text{-}tet}$ mice under ND or HFD for 6 weeks, 12 days after i.v. injection of Adeno-Adipoq (Ad-Adipoq); error bars represent SD (n=6). c: Weight of *controls* and *Fosl2* $^{ob\text{-}tet}$ mice, under ND or HFD for 6 weeks, 12 days after i.v. injection of PBS (Co), Adeno-Empty (Ad-E) or Adeno-Adipoq (Ad-Adipoq); error bars represent SD. (n=6/8). d: Fat pad/total weight of *controls* and *Fosl2* $^{ob\text{-}tet}$ mice, under ND or HFD for 6 weeks, 12 days after i.v. injection of PBS (Co), Adeno-Empty (Ad-E) or Adeno-Adipoq (Ad-Adipoq); error bars represent SD. (n=6/8). e, f: Blood glucose (e) and insulin (f) levels from *controls* and *Fosl2* $^{ob\text{-}tet}$ mice, under ND or HFD for 6 weeks, 12 days after i.v. injection of PBS (Co), Adeno-Empty (Ad-E) or Adeno-Adipoq (Ad-Adipoq); error bars represent SD. (n=6/8). g, h: Glucose tolerance (GTT) (g) and insulin tolerance (ITT) (h) tests after 6h or 3h fasting from 3 months old *controls* and *Fosl2* $^{ob\text{-}tet}$ mice, 12 days after i.v. injection of PBS (Co), Adeno-Empty (Ad-E) or Adeno-Adipoq (Ad-Adipoq) (n=6/8). Statistical analyses: *P<0.05, **P<0.01, ***P<0.001